Heliyon 9 (2023) e16231

Contents lists available at ScienceDirect

Heliyon

journal homepage: www.cell.com/heliyon

Research article

Influence of bimetal interface confinement on the Hall-petch slope of multiscale Cu/Nb multilayer composites

Chaogang Ding [a,b], Jie Xu [a,b,*], Debin Shan [a,b], Bin Guo [a,b], Terence G. Langdon [c]

[a] National Key Laboratory for Precision Hot Processing of Metals, Harbin Institute of Technology, Harbin, 150001, China
[b] Key Laboratory of Micro-systems and Micro-structures Manufacturing of Ministry of Education, Harbin Institute of Technology, Harbin 150001, China
[c] Materials Research Group, Department of Mechanical Engineering, University of Southampton, Southampton SO17 1BJ, UK

ARTICLE INFO

Keywords:
Cu-Nb
Hall-petch relationship
Interfaces
Multilayer structures
Tensile strength

ABSTRACT

Heterostructured materials afford a new way to improve the mechanical properties, which has become vital in both materials science and engineering applications. In the present research, Cu/Nb multilayer composites with layer thicknesses from the micrometer to nanometer were fabricated by accumulative roll bonding and the microstructure and mechanical properties of the Cu/Nb multilayer composites were then investigated. The yield strength and ultimate tensile strength of these composites increase with decreasing layer thickness. Moreover, the relationship between yield strength and (layer thickness)$^{-1/2}$ approximately accords with the conventional Hall-Petch equation but with a decrease in the Hall-Petch slope when the layer thickness decreases from the micrometer to nanometer scales. The deformation microstructure of these Cu/Nb multilayer composites clearly exhibit dislocations glide in the layers, which reduces the stacking of dislocations at the Cu–Nb interface and thereby weakens the strengthening effect of the interface.

1. Introduction

Recently, materials having heterostructures have attracted growing attention within the materials community [1–5]. Lamellar structured materials are important components of heterogeneous materials which have been extensively studied in experiments and the basic theory developed to describe their unique mechanical and physical properties caused by the high density of bi-metal interfaces [6–10]. Of special note is nanolayered composites where ultrahigh strength and stability, as well as functional properties, can be achieved in some nanolaminates when the individual layer thickness decreases to the nanoscale [10–14]. For example, ultra-low thermal conductivity appears when the layer thickness is below the mean free path of phonons [15] and outstanding irradiation resistance can be achieved when the individual layer thickness is below a certain critical size [16]. Therefore, nanolaminates have attracted intensive attention both from the industrial sector and from academia.

The challenges for the engineering applications of nanolaminates as structural materials arises from both the material preparation and the underlying mechanism. At present, the main fabrication methods of nanolaminates are bottom-up methods such as electrodeposition or other deposition techniques [15]. However, these deposition methods are not suitable for the preparation of bulk nanolaminates due to their high cost and the difficulty of continuous manufacturing. Recently, in the development of techniques for nanolaminate fabrication, processing by accumulative roll bonding (ARB) has effectively replaced the deposition techniques and this

* Corresponding author. National Key Laboratory for Precision Hot Processing of Metals, Harbin Institute of Technology, Harbin, 150001, China.
E-mail address: xjhit@hit.edu.cn (J. Xu).

https://doi.org/10.1016/j.heliyon.2023.e16231
Received 23 December 2022; Received in revised form 5 May 2023; Accepted 10 May 2023
Available online 12 May 2023
2405-8440/

not only reduces the cost but also permits the continuous manufacture of bulk nanolaminate materials. Nevertheless, although ARB has been used to fabricate several kinds of multilayer composites such as Cu/Nb [10,11], Cu/V [13] and Cu/Ta [17] there remains the problem that the strengthening effects of nanolaminates may be limited because the layered structures are prone to fracture [18,19]. Besides these manufacturing challenges, the strengthening mechanisms of nanolaminates are still controversial. It was reported that the mechanical response of multilayer composites at the nanometer length scale is very different from the behavior at the micrometer scale [20,21]. Moreover, three kinds of models, such as dislocation pile-up, confined layer slip and an interfaces crossing model, were developed to describe the length scale dependence of strength from the sub-micrometer to a few nanometers or less [22]. Another proposal was that the dislocations accumulate in the interface and rapidly reach a saturation density, and this indicates that the Hall-Petch relationship describes the strength even at layer thicknesses down to a few nanometers [23]. At present, many scholars have studied the strengthening behavior in nanolaminates through experiment, and found that the interface can effectively hinder the movement of dislocations and thus improve the strength of the nanolaminates [24–26]. Despite these, the mechanical response of multiscale multilayer composites from the micrometer scale down to the nanometer scale are not well-understood.

In the present research, ARB was used as a cost-effective method for fabricating bulk Cu/Nb composites with multiscale layered structures and impressively it is shown that the resultant multilayer composites exhibit continuous layered structures and excellent strength. Consequently, the present study focused on the relationship between the tensile yield strength and the layer thickness of the Cu/Nb multilayer composites, and the mechanism of the Hall-Petch slope transition behavior was investigated. It is believed that the present study can contribute to the ongoing design of multilayer composites.

2. Materials and methods

Commercial purity Cu (99.9 wt%) and Nb (99.9 wt%) sheets having dimensions of 50 × 60 × 1 mm^3 were selected as the as-received materials for this study. The raw Cu and Nb sheets were annealed under an argon gas atmosphere at temperatures of 500 °C for 1 h and 1050 °C for 1.5 h, respectively. The microstructure of pure Cu in the annealed condition consisted of equiaxed grains and twins as shown in Fig. 1(a) with an average grain size of ∼25 ± 6.5 μm. For the Nb sheets, the equiaxed grains with an average size of ∼30 ± 7.7 μm had different orientations with each other as shown in Fig. 1(b). A schematic illustration of the ARB process is given in Fig. 1(c) where there are four separate steps: (I) cleaning, (II) stacking, (III) roll bonding and (IV) cutting and annealing at 600 °C for 2 h. All multilayer composites were prepared by ARB using a mill under a rolling speed of 12 rpm at room temperature and these four steps were repeated for 15 cycles. It is worth noting that the rolling reduction of ∼78% in the first pass and ∼50% in the 2–15 cycles were selected for rolling in this work. Further details of the ARB processing are given in earlier studies [27,28]. Using this ARB process, the pure Cu and pure Nb sheets were fabricated into palm-sized Cu/Nb multilayer composites, as shown in Fig. 1(d and e).

The microstructures and chemical composition analyses were characterized by scanning electron microscopy (SEM, FEI Quanta 200FEG). The detailed microstructures of the original and fractured samples were observed using transmission electron microscopy (TEM, FEI Talos F200x). Dog bone-shaped tensile samples with nominal gauge dimensions of 5 mm × 2 mm were cut from the Cu/Nb

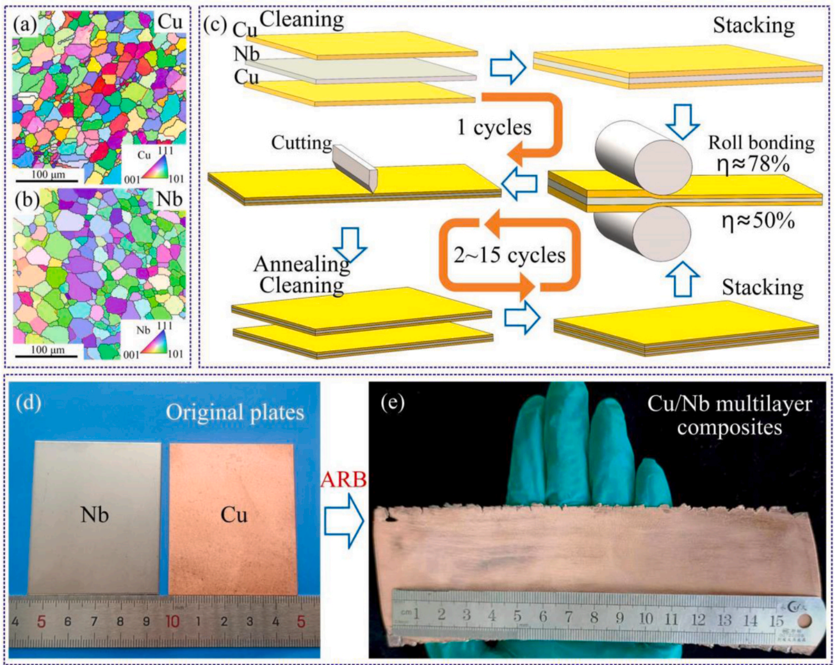

Fig. 1. The initial microstructures of (a) Cu and (b) Nb sheets. (c) Schematic illustration of the fabrication process of the Cu/Nb multilayer composites. (d) Morphologies of the Cu and Nb sheets in the present study. (e) Optical photographs of Cu/Nb multilayer composites after ARB.

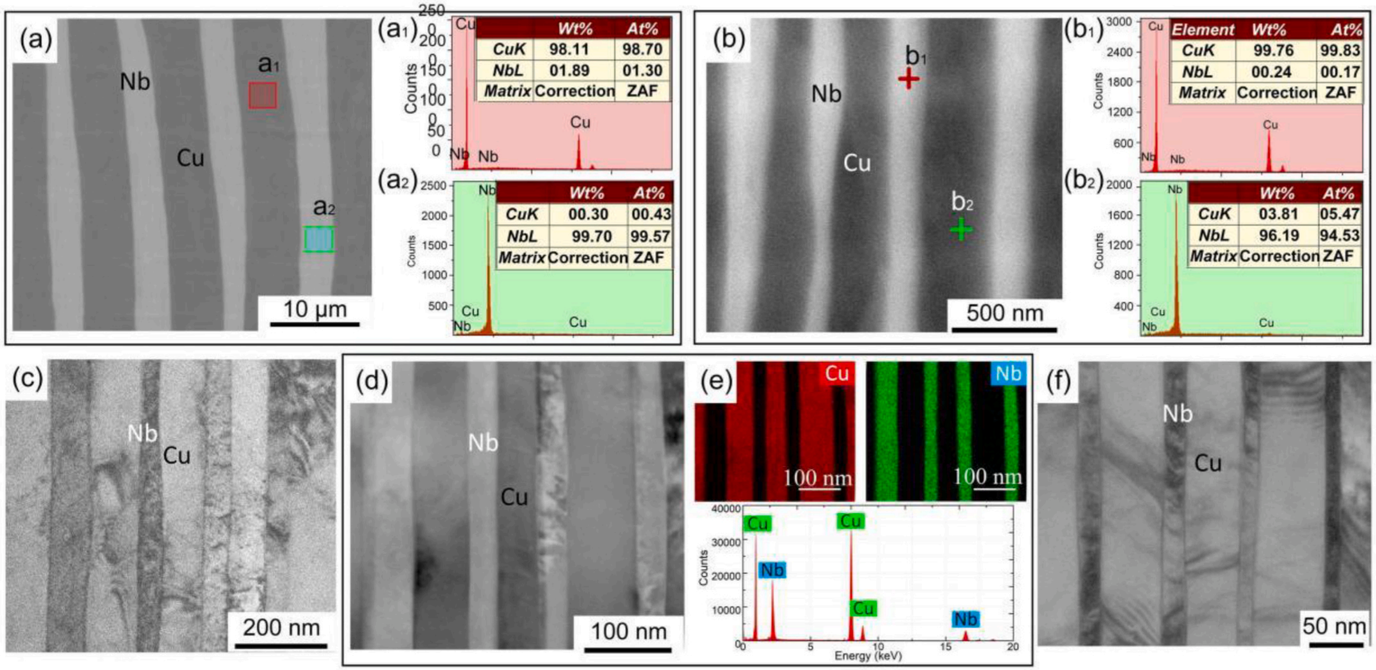

Fig. 2. Cross-section SEM morphology of the Cu/Nb multilayer composites via ARB after (a) 7 cycles, (b) 11 cycles, (a_1,a_1) and (b_1,b_2) are the corresponding EDS results in (a) and (b), respectively. Cross-section TEM images of the Cu/Nb multilayer composites after (c) 13 cycles, (d) 14 cycles, (e) the EDS elemental mapping and spectrum of (d), (f) 15 cycles.

multilayer composites using electrical discharge machining and then room temperature tensile tests were conducted using a universal materials tester (AG-X 50 kN, Shimadzu Corp.) with an initial strain rate of 2.0×10^{-4} s^{-1}. The loading direction was parallel to the rolling direction in each test and three samples of each group were tested to permit a statistical analysis of the mechanical properties.

3. Results and discussion

Fig. 2 shows the microstructures of the Cu/Nb multilayer composites after ARB processing for different numbers of cycles. The SEM and TEM micrographs reveals that the samples retain their continuous laminated structure even when the layer thickness is decreased to a few tens of nanometers length scale. As shown in Fig. 2, the thickness of the Cu layer is approximately twice that of the Nb layer which is about the same ratio as in the initial samples. This result demonstrates that the Cu/Nb multilayer composites exhibit excellent co-deformation behavior and superior structural stability during ARB processing. The BSE-SEM micrographs for the 7 and 11 cycle samples in Fig. 2(a and b) show that the interfaces are clear and without voids indicating that the Cu and Nb layers combine closely to form strongly bonded interfaces. The corresponding EDS results for the 7 and 11 cycles samples in Fig. 2(a_1,a_2) and (b_1,b_2) indicates that there was essentially no diffusion in this interfacial area. This clear interface is also observed in high magnification TEM in Fig. 2 (c), (d) and (f) after 13 to 15 cycles, respectively, and Fig. 2(e) shows the corresponding EDS elemental mapping and spectrum of the Cu/Nb multilayer composites after ARB processing for 14 cycles as in Fig. 2(d). This demonstrates that the Cu and Nb layers are alternately distributed without diffusion. The SEM-EDS and TEM-EDS results also confirm that no superfluous impurities were introduced into the composites despite experiencing so many ARB cycles.

Fig. 3(a) shows the yield strength (YS) and ultimate tensile strength (UTS) of the Cu/Nb multilayer composites processed by ARB for different numbers of cycles. As shown in Fig. 3(a), with an increase in the ARB cycles the YS and UTS of the Cu/Nb multilayer composites increases continuously. Thus, as the ARB is increased to 15 cycles the UTS of the Cu/Nb nanolaminated composites increase to 1200 MPa, where this is significantly higher than the UTS of ~354 MPa after 2 cycles and is similar to other recent studies on multilayer composites [11].

Fig. 3(b) shows the yield strength as a function of the (layer thickness)$^{-0.5}$ in the multilayer composites, where this is reasonably consistent with the Hall-Petch relationship and is similar to recent reports of tensile results in multilayer composites [10]. This indicates that the bimetal interfaces act as barriers for dislocation movement during deformation, thereby strengthening the material. In addition, nano-indentation hardness results show that the flow strength for multilayer composites at the micrometer length scale is consistent with the Hall-Petch model, while continuously increasing but deviating from the Hall-Petch relationship when the layer thickness reaches the nanometer length scale [19,22].

In this study the Hall-Petch relationship is available to estimate the strength of the multilayer composites with sub-micrometer to nanometer layer thicknesses but with a transition in the Hall-Petch slope from ~3800 MPa nm$^{1/2}$ to ~3170 MPa nm$^{1/2}$ at a layer thickness of a few micrometers length scale. This result indicates that the interfaces exhibit a weak influence on dislocation pile-up behavior when the layer thickness becomes smaller than a sub-micrometer. It has been demonstrated that the interfaces in thinner multilayer composites have a weak HP effect and a low Hall-Petch slope [19]. According to the dislocation model for multilayer composites, the change of Hall-Petch slope is ascribed to the different effects of the microstructure on dislocation motion and the mechanical response [22].

To clarify the mechanism of the dislocation motion in multilayers composites during the deformation process, microstructures of the as-prepared and tensile fractured samples were investigated in detail as given in Fig. 4. Fig. 4(a) shows that there is a low dislocation density in the as-prepared sample and Fig. 4(b) shows HRTEM images of the Cu/Nb bimetal interface. The indexing of fast Fourier transform (FFT) images and the measurement lattice spacing in Fig. 4(c and d) confirm the parallel nature of the (111)Cu and (110)Nb atomic planes along the adjacent Cu and Nb crystals with lattice spacings of 2.33 Å and 2.07 Å, respectively. Edge dislocation arrays with periodicity are found at the interfaces (as outlined by "T" in Fig. 4(b)) which compensate for the ~0.26 Å (11%) mismatch

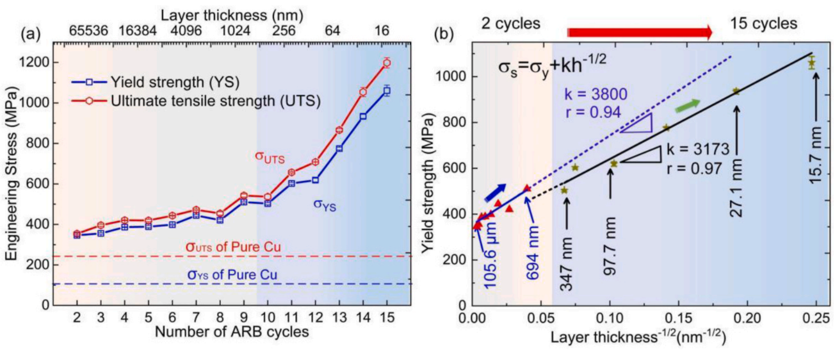

Fig. 3. (a) The yield strength and ultimate tensile strength of Cu/Nb multilayer composites processed by ARB through 2 to 15 cycles, the strength of pure Cu are included for comparison. (b) Variation of yield strength with (layer thickness)$^{-0.5}$ depicting an approximate Hall-Petch behavior, where k is the Hall-Petch slope, r is the Pearson correlation coefficient. The Hall-Page fit lines in the micrometer/nanometer range are distinguished by blue and black lines, respectively.

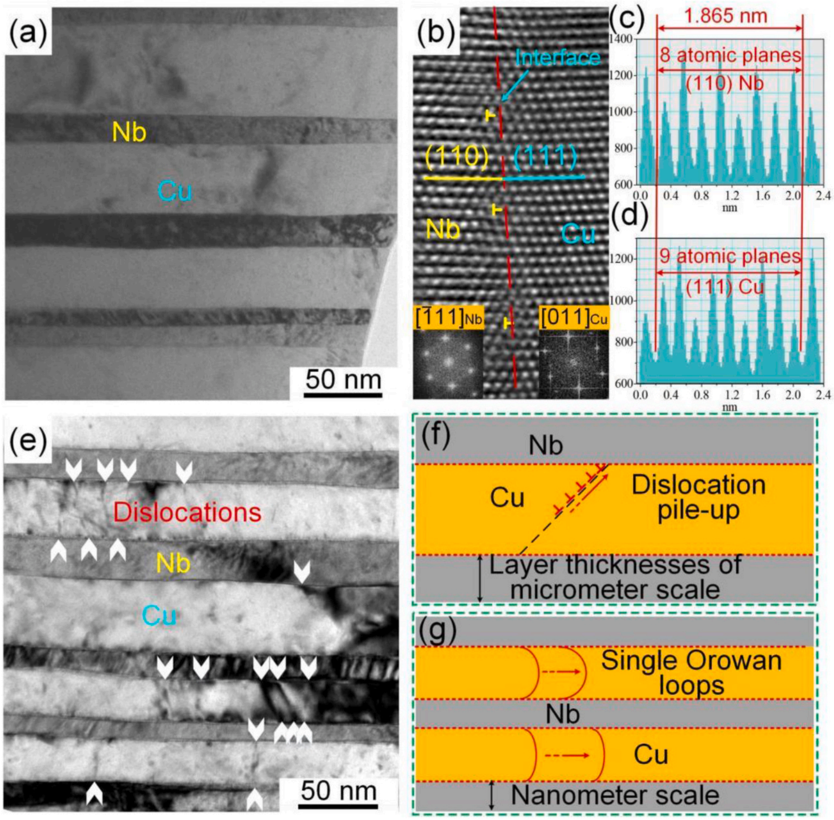

Fig. 4. (a) Bright-field TEM image of Cu/Nb multilayer composites processed by ARB through 15 cycles. (b) Typical HRTEM image of the Cu/Nb interface (insets are FFT images of both sides of the interface). (c,d) Lattice spacing of (110) plane from Nb and (111) plane from Cu were measured from HRTEM image shown in (b). (e) Microstructure of the tensile fracture samples outside of the necking region. (f) Schematic illustration of dislocation pile-up in micrometer scale multilayer composites. (g) Schematic illustration of the single Orowan loops in multilayer composites with layer thickness of a few micrometer to nanometer length scales.

between the (111)Cu and (110)Nb atomic planes.

The microstructure near the tensile fracture position of the 15 cycles Cu/Nb multilayer composites is presented in Fig. 4(e) where large quantities of dislocations (marked by white arrows) appear in both the Nb and Cu layers indicating the generation of new dislocations after deformation. Additionally, it is noteworthy that the loop-like dislocations were confined by layer interfaces, suggesting that the dislocations may propagate via an Orowan-type bowing. For layer thicknesses of the micrometer scale, the interfaces serve as barriers causing dislocation pile-ups and they contribute to multilayer composite strengthening as illustrated in Fig. 4(f). Therefore, the yield strength for multilayer composite at micrometer scales is consistent with the Hall-Petch relationship [27,29]. However, at a few micro to nanometers length scales, the interface provides the slip resistance of dislocations and forces them to bow out between the two adjacent interfaces in Cu/Nb nanolayered composites [22,30]. The glide of single dislocation loop propagation is confined to one layer and this reduces the number of dislocation pile-ups (Fig. 4(g)) thereby giving a weak Hall-Petch effect for the interfaces and leading to a smaller influence on strengthening in the multilayer composite [31,32]. Thus, the multilayer composite with layer thickness at the nanoscale shows a lower slope for the Hall-Petch relationship as in Fig. 3(b).

4. Conclusions

Multiscale Cu/Nb multilayer composites with thicknesses of micrometer to a few tens of nanometers were prepared by ARB processing. The excellent co-deformation behavior of the two layers guarantees that the laminated structure remains continuous. The composites exhibit a sufficiently high tensile strength of 1.20 GPa and the yield strength approximately follows the Hall-Petch relationship for the layer thickness. However, there is a transition in the Hall-Petch slope at layer thicknesses of a few micrometers length scale. Dislocation glide was confined by the interfaces to occur within each layer, resulting in a reduction in the number of dislocation pile-ups and giving rise to a weak effect of the interfaces.

Author contribution statement

Chaogang Ding: Conceived and designed the experiments; Performed the experiments; Analyzed and interpreted the data; Contributed reagents, materials, analysis tools or data; Wrote the paper.

Jie Xu: Conceived and designed the experiments; Performed the experiments; Analyzed and interpreted the data; Contributed reagents, materials, analysis tools or data.

Debin Shan, Bin Guo: Conceived and designed the experiments; Analyzed and interpreted the data.

Terence G. Langdon: Conceived and designed the experiments; Analyzed and interpreted the data; Wrote the paper.

Data availability statement

Data will be made available on request.

Declaration of competing interest

The authors declare that they have no known competing financial interests or personal relationships that could have appeared to influence the work reported in this paper.

Acknowledgement

This work was supported by the National Natural Science Foundation of China under Grant No. 51635005 and the Program of Introducing Talents of Discipline to Universities under grant number B18017. Partial support was provided by the European Research Council under ERC Grant Agreement No. 267464-SPDMETALS (TGL).

References

[1] X. Wu, Y. Zhu, K. Lu, Ductility and strain hardening in gradient and lamellar structured materials, Scripta Mater. 186 (2020) 321–325.
[2] L.J. Huang, L. Geng, H. Peng, Microstructurally inhomogeneous composites: is a homogeneous reinforcement distribution optimal? Prog. Mater. Sci. 71 (2015) 93–168.
[3] H. Teng, Y. Jiang, Z. Tan, P. Liu, G. Fan, D. Xiong, Z. Li, Towards an atomic-scale understanding of interface characteristics in graphene/Al composites, Mater. Today Commun. 33 (2022), 104240.
[4] L.G. Sun, G. Wu, Q. Wang, J. Lu, Nanostructural metallic materials: structures and mechanical properties, Mater, Today Off. 38 (2020) 114–135.
[5] W. Zhao, H. Liao, Y. Lun, S. Zhang, B. Song, Role of interfaces in the deformation behavior of lamellar TiAl-based alloys with CPFEM simulation, Mater. Today Commun. 32 (2022), 103942.
[6] W. Yang, I.J. Beyerlein, Q. Jin, H. Ge, T. Xiong, L. Yang, J. Pang, Y. Zhou, X. Shao, B. Zhang, S. Zheng, X. Ma, Strength and ductility of bulk Cu/Nb nanolaminates exposed to extremely high temperatures, Scripta Mater. 166 (2019) 73–77.
[7] A. Biradar R. M, Evolution of microstructure and mechanical properties for multi-layered Al-1100 strips and Al-Gr composites fabricated by accumulative roll bonding, Mater. Today Commun. 34 (2023), 105027.
[8] M. Cao, F. Jiang, R. Zhou, R. Qin, H. Zhang, Z. Wang, C. Guo, A novel bio-inspired metal hollow sphere filled TC4/Al sandwich composite: fabrication and compressive properties, Mater, Today Commun 31 (2022), 103349.
[9] Y. Xia, H. Wu, K. Miao, X. Li, C. Xu, L. Geng, H. Xie, G. Fan, Effects of the layer thickness ratio on the enhanced ductility of laminated aluminum, J. Mater. Sci. Technol. 111 (2022) 256–267.
[10] T. Nizolek, I.J. Beyerlein, N.A. Mara, J.T. Avallone, T.M. Pollock, Tensile behavior and flow stress anisotropy of accumulative roll bonded Cu-Nb nanolaminates, Appl. Phys. Lett. 108 (2016), 51903.
[11] R. Gao, M. Jin, F. Han, B. Wang, X. Wang, Q. Fang, Y. Dong, C. Sun, L. Shao, M. Li, J. Li, Superconducting Cu/Nb nanolaminate by coded accumulative roll bonding and its helium damage characteristics, Acta Mater. 197 (2020) 212–223.
[12] W. Yang, M. Gong, J. Yao, J. Wang, S. Zheng, X. Ma, Hardening induced by dislocation core spreading at disordered interface in Cu/Nb multilayers, Scripta Mater. 200 (2021), 113917.
[13] L.F. Zhang, R. Gao, J. Hou, L.F. Zeng, J.J. Xin, X.B. Wu, X.P. Wang, Q.F. Fang, C.S. Liu, The effects of interfaces stability on mechanical properties, thermal conductivity and helium irradiation of V/Cu nano-multilayer composite, Mater. Des. 216 (2022), 110535.
[14] M. Nasim, Y. Li, M. Wen, C. Wen, A review of high-strength nanolaminates and evaluation of their properties, J. Mater. Sci. Technol. 50 (2020) 215–244.
[15] L. Dong, G. Wei, T. Cheng, J. Tang, X. Ye, M. Hong, L. Hu, R. Yin, S. Zhao, G. Cai, Y. Shi, B. Pan, C. Jiang, F. Ren, Thermal conductivity, electrical resistivity, and microstructure of Cu/W multilayered nanofilms, Acs Appl. Mater. Inter. 12 (2020) 8886–8896.
[16] W. Han, M.J. Demkowicz, N.A. Mara, E. Fu, S. Sinha, A.D. Rollett, Y. Wang, J.S. Carpenter, I.J. Beyerlein, A. Misra, Design of radiation tolerant materials via interface engineering, Adv. Mater. 25 (2013) 6975–6979.
[17] L.F. Zeng, R. Gao, Q.F. Fang, X.P. Wang, Z.M. Xie, S. Miao, T. Hao, T. Zhang, High strength and thermal stability of bulk Cu/Ta nanolamellar multilayers fabricated by cross accumulative roll bonding, Acta Mater. 110 (2016) 341–351.
[18] H.S. Shahabi, M. Eizadjou, H.D. Manesh, Evolution of mechanical properties in SPD processed Cu/Nb nano-layered composites, Mater. Sci. Eng., A 527 (2010) 5790–5795.
[19] T. Mungole, B. Mansoor, G. Ayoub, D.P. Field, Bifurcation in deformation behavior of Cu and Ta by accumulative roll-bonding at high temperature, Scripta Mater. 136 (2017) 87–91.
[20] M. Jain, K. Yaddanapudi, A.T. Kidigannappa, K. Baldwin, M. Knezevic, N.A. Mara, I.J. Beyerlein, S. Pathak, Simultaneous high strength and mechanical stability of bcc Nb/Mg nanolaminates, Acta Mater. 242 (2023), 118487.
[21] J. Wang, A. Misra, An overview of interface-dominated deformation mechanisms in metallic multilayers, Curr. Opin. Solid. St. M. 15 (2011) 20–28.
[22] A. Misra, J.P. Hirth, R.G. Hoagland, Length-scale-dependent deformation mechanisms in incoherent metallic multilayered composites, Acta Mater. 53 (2005) 4817–4824.
[23] S. Subedi, I.J. Beyerlein, R. LeSar, A.D. Rollett, Strength of nanoscale metallic multilayers, Scripta Mater. 145 (2018) 132–136.
[24] Y. Zhang, N. Li, M.M. Schneider, T.J. Nizolek, L. Capolungo, R.J. McCabe, Kink mechanism in Cu/Nb nanolaminates explored by in situ pillar compression, Acta Mater. 237 (2022), 118150.
[25] C. Ding, J. Xu, D. Shan, B. Guo, T.G. Langdon, The thermal instability mechanism and annealed deformation behavior of Cu/Nb nanolaminate composites, J. Mater. Sci. Technol. 157 (2023) 163–173.

[26] Y. Zhang, J.G. Gigax, T.J. Nizolek, J.S. Carpenter, M.M. Schneider, N. Li, L. Capolungo, R.J. McCabe, Tensile and failure behaviors of Cu/Nb nanolaminates: the effects of loading direction, layer thickness, and annealing, Acta Mater. 240 (2022), 118346.
[27] C. Ding, J. Xu, X. Li, D. Shan, B. Guo, T.G. Langdon, Microstructural evolution and mechanical behavior of Cu/Nb multilayer composites processed by accumulative roll bonding, Adv. Eng. Mater. 22 (2020), 1900702.
[28] C. Ding, J. Xu, D. Shan, B. Guo, T.G. Langdon, Sustainable fabrication of Cu/Nb composites with continuous laminated structure to achieve ultrahigh strength and excellent electrical conductivity, Compos. B Eng. 211 (2021), 108662.
[29] J.Y. Zhang, K. Wu, L.Y. Zhang, Y.Q. Wang, G. Liu, J. Sun, Unraveling the correlation between Hall-Petch slope and peak hardness in metallic nanolaminates, Int. J. Plast. 96 (2017) 120–134.
[30] J. Wang, M. Knezevic, M. Jain, S. Pathak, I.J. Beyerlein, Role of interface-affected dislocation motion on the strength of Mg/Nb nanolayered composites inferred by dual-mode confined layer slip crystal plasticity, J. Mech. Phys. Solid. 152 (2021), 104421.
[31] M.F. Tambwe, D.S. Stone, A.J. Griffin, H. Kung, Y. Cheng, M. Nastasi, Haasen plot analysis of the Hall-Petch effect in Cu/Nb nanolayer composites, J. Mater. Res. 14 (1999) 407–417.
[32] T. Chen, R. Yuan, I.J. Beyerlein, C. Zhou, Predicting the size scaling in strength of nanolayered materials by a discrete slip crystal plasticity model, Int. J. Plast. 124 (2020) 247–260.